LA-UR- 09-00195

Approved for public release;
distribution is unlimited.

Title:	Development of Membranes for Hydrogen Separation: Pd-coated V-10Pd
Author(s):	Stephen N. Paglieri, LANL Joseph R. Wermer, LANL Robert E. Buxbaum, REB Research & Consulting Michael V. Ciocco, NETL Bret H. Howard, NETL Bryan D. Morreale, NETL
Intended for:	Energy Materials

Los Alamos
NATIONAL LABORATORY
EST. 1943

Form 836 (7/06)

Development of Membranes for Hydrogen Separation: Pd-coated V-10Pd

Stephen N. Paglieri[1], Joseph R. Wermer[1], Robert E. Buxbaum[2], Michael V. Ciocco[3], Bret H. Howard[4], Bryan D. Morreale[4]

[1]Los Alamos National Laboratory, P.O. Box 1663 MS-C927, Los Alamos, New Mexico, USA
E-mail: steve.paglieri@lanl.gov; Telephone: (505) 667-0652; Fax (505) 665-1226

[2]REB Research and Consulting, Ferndale, MI, USA
REB Research & Consulting, 3259 Hilton Rd., Ferndale, MI 48220
E-mail: buxbaum@rebresearch.com; Telephone: (248) 545-0155; Fax: (248) 545-5430

[3]National Energy Technology Laboratory, Parsons; P.O. Box 618, South Park, PA, 15129
E-mail: Michael.Ciocco@pp.netl.doe.gov; Telephone: (412) 386-4711

[4]National Energy Technology Laboratory, Pittsburgh, PA, USA
P.O. Box 10940, Pittsburgh, PA 15236-0940
E-mail: Bret.Howard@ netl.doe.gov; Telephone: (412) 386-5908; Fax: (412) 386-5920

Abstract

Numerous Group IVB and VB alloys were prepared and tested as potential membrane materials but most of these materials were brittle or exhibited cracking during hydrogen exposure. One of the more ductile alloys, V-10Pd (at.%), was fabricated into a thin foil (107-μm thick) composite membrane coated with 100 nm of Pd on each side. The material was tested for hydrogen permeability, resistance to hydrogen embrittlement, and long term hydrogen flux stability. The hydrogen permeability, Φ, of the V-10Pd membrane was 3.86×10^{-8} mol H_2 m^{-1} s^{-1} $Pa^{-0.5}$ (avg. of three different samples) at 400°C, which is slightly higher than the permeability of Pd-23Ag at that temperature. A 1400 h hydrogen flux test at 400°C demonstrated that the rate of metallic interdiffusion was slow between the V-10Pd foil and the 100-nm-thick Pd coating on the surface. However, at the end of testing the membrane cracked at 118°C because of hydrogen embrittlement.

keywords: hydrogen permeability, hydrogen flux, vanadium alloy membrane, palladium, embrittlement,

1. Introduction

More efficient consumption of energy resources is important to conserve limited supplies, reduce pollution, and minimise the harmful effects of global climate change. Integration of membranes into hydrogen separating processes may improve the efficiency of hydrogen production and utilisation. There are many situations where durable and cost effective hydrogen separating membranes can contribute to improving energy intensive processes.[47] For example, most of the hydrogen produced worldwide is created by steam reforming of methane using natural gas as a feedstock. Traditionally, the hydrogen produced by this method is purified using pressure swing adsorption that produces > 99.9% pure hydrogen. By far, the largest consumer of hydrogen is refineries for hydrocracking and hydrodesulfurisation of fuels. However, for hydrogen to be used in Polymer Electrolyte Membrane fuel cells (PEMFC), the CO content must be significantly less than 1 ppm to avoid poisoning the Pt-containing electrodes. Defect-free metal membranes can be used to produce hydrogen with < 1 ppb impurities. Furthermore, hydrogen may be produced more economically than conventional processes in membrane reactors that integrate catalytic generation and separation of hydrogen or by using reactors that extract hydrogen with interstage membranes.[13, 18, 28, 57]

A large fraction of the electrical power in the United States and the rapidly developing world (particularly China and India) is generated in centralised power plants that burn coal. Environmentally sustainable use of this cheap and abundant fuel is

imperative until the costs of harvesting and storing renewable energy are decreased through technological innovations. A more carbon-neutral scheme has been proposed that involves integrated gasification combined-cycle (IGCC), with co-generation of electricity and hydrogen, chemicals, or liquid fuels. Carbon sequestration involves capture and geological storage of the residual waste gas containing high concentrations of carbon-dioxide.[38] Catalytic membrane reactors may be used to produce hydrogen through shift reaction of gasified coal, increasing the overall hydrogen yield of this process.[14, 28] The required hydrogen separating membranes must withstand the conditions (high temperatures and pressures) and gases (various carbon and sulfur species) present in gasified coal. Membranes must also be affordable, compact, durable, have high hydrogen flux, and last for many years.

Metal membranes composed of Pd–Ag or Pd–Cu foils or tubes are presently used to obtain ultra-high-purity hydrogen for laboratory use, compound semiconductor manufacturing,[36] tritium (^{3}H) purification,[18] and hydrogen isotope extraction from nuclear reactors.[63, 65] Most commercial hydrogen purification units contain conventional metal membrane technology consisting of relatively thick (> 20 μm) Pd alloy foil or tubular membranes that are costly because of the precious metal content. Composite membranes with thin films of Pd alloy supported on porous substrates greatly reduce precious metal content but typically have high fabrication cost because of the multi-step preparation method or because of the cost of the engineered porous support.[46, 52] Cost and durability issues prevent Pd-based metal membranes from being used more extensively for large-scale hydrogen separations or in membrane reactors for hydrogen generation or chemical production.[18] Consequently, membranes are under development based on Group

IVB and VB elements that have high hydrogen permeabilities because of their body-centered-cubic (bcc) structure.[1, 3, 4, 11, 37, 39, 43, 44, 49, 62, 67, 72] Amorphous alloy membranes are another promising area for hydrogen separations.[14]

Despite their significantly lower cost, Group IVB and VB metal membranes have not replaced Pd alloys for several reasons. First, metals such as V and Nb with high hydrogen permeability often have high hydrogen solubility and are prone to fracture because of the formation of brittle hydride phases.[17, 30, 45, 70] Hydrogen absorption causes the material to expand and the resulting stress causes membrane failure. Alloying elements can increase the ability of the metal to absorb hydrogen without the formation of lattice-expanding hydride phases whereupon ductility rapidly decreases and embrittlement occurs.[6, 54, 55, 66, 67] For example, Pd and Pd-alloy coated V-Ni alloys and some ternary alloys based on V-Ni have been investigated extensively, demonstrating their high hydrogen permeability and alleged resistance to hydrogen embrittlement.[3, 41, 42, 44, 75, 76] Ternary composition, multi-phase alloys consisting of a ductile phase that helps maintain membrane integrity and a brittle phase with high hydrogen permeability have been shown to possess both acceptable hydrogen permeability and increased durability.[19, 33] For example, alloys such as (V, Nb, Ta)-Ti-Ni, and Ti-Ni-Pd have hydrogen permeabilities comparable to Pd-23Ag and resist embrittlement to temperatures as low as 150°C.[4, 26, 33]

Unlike Pd and its alloys, the catalytic properties for hydrogen dissociation of Group IVB and VB metal surfaces are substantially diminished by the presence of a tenacious oxide layer.[22, 69] Accordingly, surface oxide layers are removed from these metals by either mechanical abrasion, chemical etching, or ion milling and a thin Pd or Pd alloy coating is applied to both sides of a membrane to promote dissociation of hydrogen

molecules on the upstream side and re-association on the downstream side of the membrane.[5, 11, 16, 24, 31, 32, 34, 37, 40, 50, 51] The thickness of Pd coating required on Group IVB and VB membranes is generally much thinner (< 1 μm per side) than freestanding or supported Pd-alloy membranes.[47]

However, during exposure to hydrogen at temperatures above 400°C, the Pd coating may undergo delamination from the surface[53] or interdiffuse with the base membrane material resulting in decreased hydrogen permeability over time.[16] As the Pd content at the surface decreases, so does the catalytic activity for hydrogen dissociation and as the reactive base metal becomes exposed or its alloy constituents diffuse to the surface they may be oxidised, blocking hydrogen dissociation and permeation through the membrane.[20] It follows that thicker Pd coatings will prolong composite membrane functional operating lifetime.[9, 16] Furthermore, alloys of V may be more oxidation resistant. Barrier layers are being developed that prevent metallic interdiffusion between the Pd coating and the membrane while maintaining high hydrogen permeability.[16, 21, 73]

Another important issue is manufacturability.[15] Other than higher hydrogen permeability, some of the potential advantages of V alloys over Pd alloys include better high temperature tensile strength and creep properties. Presently, studies of Group IVB and VB membranes have been conducted primarily on relatively thick foils. Therefore, methods will have to be devised for fabricating modules consisting of tubular or thin foil membranes. With this in consideration, alloys of these membrane materials must be ductile enough to roll into foil or draw into tube. Special welding and joining techniques must also be developed that take into account the reactive nature of these materials.[59, 61] Advancements in viable processes for deposition of ultra thin, large area Pd alloy

coatings are also necessary, probably including electro- and electroless plating, and physical vapor deposition.[11, 35, 37, 46, 49, 68]

The objective of the present work was to investigate the properties of the V-10Pd alloy as a potential membrane material. By alloying V with Pd, it was anticipated that the durability of the material in hydrogen would be increased while maintaining the high hydrogen permeability characteristic of V. We evaluated the hydrogen permeability of Pd/V-10Pd/Pd composite membranes and other properties such as long term thermal stability to demonstrate that the V-10Pd alloy has improved properties for membrane applications compared to pure V.

2. Hydrogen Permeation through Metal Membranes

According to Sieverts' law, hydrogen concentration in a metal is described by:

$$C = K_s P^n, \tag{1}$$

where K_s is Sieverts' constant or solubility and P is the partial pressure of hydrogen at equilibrium with the metal surface.[58] The exponent n is equal to 0.5 when permeation is controlled by atomic hydrogen permeation through the bulk metal.[25, 64] Permeability is the product of solubility and diffusivity of hydrogen in the metal:

$$\Phi = K_s D. \tag{2}$$

Steady state hydrogen flux, J, through a metal membrane is driven by the hydrogen concentration difference on opposite sides of the membrane:

$$J = D(C_r - C_p)l^{-1} \tag{3}$$

Here, l is membrane thickness, and C_r and C_p are the partial pressures of hydrogen on the retentate (upstream) and permeate (downstream) sides of the membrane. Flux is generally expressed by the following equation by utilising Eqs. (1-3):

$$J = \Phi(P_r^n - P_p^n)l^{-1}. \quad (4)$$

Permeability is determined from a series of steady state flux measurements over a range of pressures and the apparent activation energy for hydrogen permeability is calculated from permeation values at several temperatures.

3. Experimental

3.1 Alloy and Membrane Preparation

High purity metals were melted into buttons in an arc furnace. The buttons were flipped and re-melted to ensure compositional uniformity. A button of V-10Pd was sliced and rolled into a sheet with a nominal thickness of 0.107 mm. The foil was washed with warm water and soap, rinsed with methanol, blown dry with nitrogen, mounted by clamping the ends of the foil strip, and loaded into the physical vapor deposition (PVD) chamber. After evacuation of the chamber to ~1×10^{-5} Pa, argon was bled into the chamber to a pressure of 2×10^{-2} Pa and the ion-gun was set to a power of 1 keV and 20-25 mA to ion-mill each side of the foil for 60-90 min. The foil was visually inspected through a window during ion-milling to ensure removal of remaining surface contaminants. After ion-milling, argon was evacuated from the chamber and Pd was *e*-beam evaporated onto each side of the foil to a thickness of 100 nm at 3-5 Å/s. A quartz crystal was used to monitor the thickness of metal deposited.

3.2 Hydrogen Permeability Testing

The Pd-coated V-10Pd foil was cut into 19-mm diameter discs. A composite membrane disc was sandwiched between two Ag-plated Ni VCR gaskets (12.7 mm ID) and positioned in the fixture, a stainless steel VCR fitting adapted with an impinging flow design. The mated fixture was tightened roughly one-quarter turn. The membrane surface area was 0.94 cm^2. A typical membrane after hydrogen flux testing is shown in Fig. 1. The membrane module was placed in a furnace and connected to a gas supply and measurement system. Helium pressurisation tests were performed to confirm the absence of leaks. Helium and argon were nominally 99.9995% pure and hydrogen was 99.99995% pure and both gases were used without further purification. Mass flow controllers metered the gas flows while 0-1330 kPa, 0-13.3 kPa, and 0-1.33 kPa pressure transducers measured upstream (retentate) and downstream (permeate) pressures.

The membrane module was heated in the absence of hydrogen with an argon purge on the retentate side and argon purge or vacuum (provided by an oil-free turbomolecular pump backed by a scroll pump) on the permeate side of the membrane. The hydrogen feed pressure ranged between 101-355 kPa and the permeate pressure ranged between 0.5-103 kPa. Pressures were controlled using back-pressure regulators. Sweep gas was not used during the permeation experiments. Hydrogen flux was measured using calibrated flowmeters. Hydrogen permeation tests were also conducted on a 0.250-mm-thick Pd-23Ag foil and a Pd-coated (100 nm) 0.375-mm-thick V foil.

3.3 Alloy and Membrane Characterisation

Charpy indentation tests were performed on as-prepared alloy buttons before and

after exposure to hydrogen as a semi-quantitative measure of ductility. Higher values are indicative of greater ductility. Pd-coated composite membranes were prepared from some of the alloys that were not too brittle as cast and tested for hydrogen permeability. Membranes were examined using an Aspex PSEM 2000 equipped with EDS prior to and following hydrogen flux testing to determine micro-scale morphological changes such as those in the Pd coating and alloy grains. A PANalytical X'Pert Pro MPD powder diffractometer having a theta-theta configuration, a copper X-ray source operated at 45 kV and 40 mA and an X'Celerator detector with a monochromator was used to determine crystalline phases present in the membranes and changes resulting from flux testing. Patterns were typically recorded over a 2θ range of 10 to 100°.

4. Results and Discussion

4.1 New Alloy Development

A series of Group IVB and VB based alloys substituted with various transition metals were prepared and cut or rolled into membrane discs.[7, 8, 10] The three primary criteria for selecting new alloys that were considered included as-cast ductility (workability), hydrogen permeability, and resistance to hydrogen embrittlement. For the most part, brittle alloys were not coated with Pd and tested for hydrogen permeability. Some of the materials that showed potential are listed in Table 1. Our results differ from those obtained previously by other researchers[44] in that the V-Ni-Al alloy was not workable enough to form into a membrane for hydrogen permeability testing.

Additional alloys that were less promising as hydrogen separating membranes are listed in the Appendix. The V-10Pd alloy was selected for further investigation because

of its potential based on good ductility and reasonable hydrogen permeability. Most alloys were brittle as cast and embrittled further upon hydrogen exposure even though phase diagrams were consulted to avoid regions where brittle intermetallics are expected to form instead of substitutional alloys. However, the composition V-10Pd is in the solid solution range,[60] enabling a thin (~0.1 mm) foil to be rolled.

4.2 V-10Pd Membrane Characterisation

XRD patterns for Pd-coated V-10Pd alloy membranes that were untested or hydrogen permeation tested are shown in Fig. 2. Only peaks assignable to V and Pd were detected. An unidentified peak was associated with the coating, since it did not appear in XRD patterns of the alloy without the Pd coating. The V peak shifted slightly suggesting the formation of an alloy, which was expected considering up to 20at.% Pd is soluble in V.[60] The Pd peaks on the untested composite membrane were broadened because the Pd was deposited by physical vapor deposition, probably resulting in residual stress in the coating. After annealing for a few days at 400°C in hydrogen, the Pd peaks had narrowed because of crystallisation of the surface coating. Comparison of tested and untested samples showed no assignable differences in terms of phase or composition changes.

Back scattered electron SEM images of the Pd-coated V-10Pd membrane surface before and after testing are shown in Fig. 3a-c. The surface of the Pd-coated V-10Pd foil was fairly smooth with some texture and scratches from cold rolling. As shown in Fig. 3b, in some places the 100-nm-thick Pd coating delaminated from the foil, however, it was estimated that such bare patches comprised < 2% of the total surface area of the membrane. Fig. 3c shows the surface of the membrane after testing in hydrogen for 162 h

at 400°C. The membrane surface appeared to be rougher after this extended testing period probably because of grain growth in the Pd coating as evidenced by peak narrowing in the XRD results (see Fig. 2). In conjunction with the apparent roughening due to the grain growth of the Pd coating, areas having a thinner Pd coating are expected. The darker gray regions in Fig. 3c are likely due to these thin areas.

4.3 Hydrogen Permeation Measurements

The hydrogen flux measured through a V-10Pd membrane over a range of pressures at 400°C is shown in Fig. 4, including flux data for V and Pd-23Ag membranes. It is evident that V is highly permeable, since the flux was much higher than through the other membranes even though it was 3.5 times as thick as the V-10Pd membrane and 1.3 times thicker than the Pd-23Ag membrane. Furthermore, the thickness normalised flux through the V-10Pd membrane would be comparable to the Pd-23Ag membrane considering the V-10Pd membrane was less than half as thick.

The temperature dependence of hydrogen permeability for the V, V-10Pd, and Pd-23Ag membranes is shown in Fig. 5. Hydrogen permeabilities were determined from data similar to that shown in Fig. 4 and by using equation (4) they were derived from hydrogen flux measurements over a range of pressures and temperatures between 200-500°C at 25°C intervals. The data was fit to equation (4) using an n-value of 0.5 and minimised R^2 values of > 0.98 were obtained at almost all temperatures. This implied that the rate limiting step for hydrogen permeation through the membrane was bulk diffusion and not the rate of hydrogen dissociation on the surface. It is evident from Fig. 5 that the hydrogen permeability of V was higher than both V-10Pd and Pd-23Ag. However, the

permeability of V-10Pd was lower than Pd-23Ag, except above 375°C. Our permeability for Pd-23Ag is in good agreement with that of Serra et al.[56] The data for the pure V membrane was limited because it cracked due to hydrogen embrittlement at 375°C and at temperatures ≥ 400C, metallic interdiffusion between V and the Pd coating resulted in a rapid decrease hydrogen flux. Important membrane parameters are compiled in Table 2 for comparison.

Apparent activation energies for hydrogen permeation were obtained from this Arrhenius type plot (Fig. 5) although the variation with temperature was not completely linear for V-10Pd.[12] The activation energy for hydrogen permeation through the V-10Pd membrane at < 400°C as determined from Fig. 5 was 38.8 kJ/mol (average of two different membranes), which is at the higher limit of the results obtained by Katsuta for pure V of 24-39 kJ/mol.[29] Our activation energy obtained for pure V was also within this range (28.0 kJ/mol).The slope in permeability of the V-10Pd membrane leveled off so that the activation energy at ≥ 400°C was 12.9 kJ/mol (average of two different membranes), which was closer to that of Pd-23Ag (10.8 kJ/mol), possibly indicating a change in diffusion mechanism above 400°C. It is possible that the properties of the Pd coating have a greater influence above this temperature as both the rate of hydrogen dissociation on the surface and rate of hydrogen permeation through the Pd coating increase at higher temperature.

4.4 Long Term Hydrogen Flux Test

A long term hydrogen flux test was conducted to observe any changes because of interdiffusion between the 100 nm Pd coating with the V-10Pd membrane. The results for

a 1400 h test at 673 K are shown in Fig. 6. The flux through the composite Pd/V-10Pd membrane was fairly constant for the duration of the test (after an initial period of equilibration) with only a slight decrease in flux towards the end of the test. Alloy constituents of the base membrane can diffuse to the surface and can be oxidised, reducing permeability.[23] This mechanism of membrane degradation and resulting flux decrease in hydrogen flux has been observed previously with Pd-coated V, Ta, V-Ti, and V-6Ni-5Co membranes.[11, 16, 20, 27, 48] It is likely that this mechanism is also occurring here and by the end of the test period may be beginning to cause a noticeable flux decline. Also, recrystallisation of the Pd coating, as noted in Section 4.2 for a membrane tested for only 162 hours, could also be affecting long term performance.

4.5 Mechanical Stability in Hydrogen

For this test, the temperature was reduced at 1°C/min with hydrogen on the retentate side at a pressure of 101 kPa while the permeate side of the membrane was evacuated. The temperatures and pressures where hydrogen broke through each type of membrane are shown in Table 3. A 0.250-mm-thick Pd-23Ag membrane withstood exposure to hydrogen at 25°C without rupturing. In contrast, a 0.040-mm-thick pure V membrane broke at 262°C whereas a 0.107-mm-thick V-10Pd membrane failed at 118°C under the same condition of a 97 kPa pressure drop across the membrane in hydrogen. Another V-10Pd membrane failed in hydrogen at 150°C at a slightly higher pressure differential (110 kPa). It seems that the V-10Pd alloy is much more resistant to hydrogen embrittlement than pure V. However, it should be noted that this test was only a qualitative comparison of membrane durability since factors such as thickness and testing history likely influence

the outcome. Also, constraining the membrane in a planar configuration imparts considerable stress during hydrogen absorption and the resulting dilatation.[2, 74] After testing, membranes were often observed to have been bowed slightly toward the permeate side.

5. Summary and Conclusions

Numerous Group IVB and VB alloys were prepared but very few were ductile enough to be used as potential membrane materials, especially when exposed to hydrogen. Some of the more ductile alloys were screened for their hydrogen permeability and resistance to hydrogen embrittlement. The V-10Pd alloy exhibited higher hydrogen permeability than Pd-25Ag at higher temperatures (> 375°C), and exhibited a slow rate of metallic interdiffusion with its thin Pd coating during long term testing at 400°C. Despite increased resistance to hydrogen embrittlement compared to pure V, the V-10Pd alloy still fractured in hydrogen at 118°C. Therefore, further investigation on variations of this alloy or others is necessary to find a hydrogen permeable material that is durable enough for industrial applications.

Acknowledgments

Alloys were prepared at the Ames Laboratory Material Preparation Center by Dr. Alan M. Russell. The authors are grateful to R. C. Snow for performing PVD, and Dr. H. Oona, B. Roybal, T. Shevin, C. T. Howard, H. M. Murdock, and B. P. Nolen for experimental setup and data collection. This research was supported by the U.S. Department of Energy.

List of Figure Captions

Figure 1. A typical composite membrane disc sealed between two Cu VCR gaskets (Ni gaskets are normally used). This 0.37-mm thick V-6Ni-5Co membrane (coated with 100 nm Pd per side) was tested for 170 h at 450°C.[48]

Figure 2. XRD patterns for Pd-coated (100 nm) V-10Pd membranes before and after testing at 400°C for 162 h.

Fig. 3. Surface of the Pd-coated (100 nm) V-10Pd membrane before (a, b) and after (c) testing in hydrogen for 162 h at 400°C showing: the surface texture (a); a spot (< 2% of the total surface area) where Pd delaminated from the surface (b); and the increase in surface roughness during testing (c).

Figure 4. Hydrogen flux dependence on pressure at 400°C through three different samples of 0.107-mm-thick Pd-coated (100 nm) V-10Pd membrane, a Pd-coated (100 nm) 0.375-mm-thick V membrane, and a 0.250-mm-thick Pd-23Ag membrane.

Figure 5. Temperature dependence of hydrogen permeabilities for Pd-coated (100 nm) V, two different Pd-coated (100 nm) V-10Pd membranes, and a Pd-23Ag membrane.

Figure 6. Long term hydrogen flux test for a 0.107-mm-thick Pd-coated (100 nm) V-10Pd membrane at 400°C. The pressure of hydrogen on the retentate side of the membrane was 101 kPa and the pressure on the permeate side was 0.6 kPa.

List of Tables

Table 1. Some alloys that were ductile enough to be tested for hydrogen permeability

Alloy (at.%)	As-cast workability	Critical strain	Hydrogen permeability ($mol/m \cdot s \cdot Pa^{0.5}$)	Embrittles in hydrogen?	Hydrided critical strain
Pd-23Ag	very ductile	not measured	moderate: 2.52×10^{-8}	No: can be exposed to hydrogen at room temperature	not measured
V	ductile	> 0.026	high: 3.62×10^{-7}	severely at < 300°C	0.0036
V-10Pd	moderately ductile: was rolled into 0.11 mm-thick foil	> 0.019	higher than Pd-23Ag: 3.86×10^{-8}	yes, at temperatures < 150°C	0.0016
V-9Ni	somewhat brittle	> 0.017	8.5×10^{-8}	yes	0.002
V-5Ti	ductile	not measured	high	yes, at ~300°C	not measured
V-15Cu	ductile	not measured	high	yes, at ~350°C	not measured
V-6Ni-5Co, V-9Ni-3Co	hard to roll	0.022	5.3×10^{-8}	fails at < 200°C	0
Co-25V	ductile	not measured	0	no	not measured
Co-25Ti Co-50Ti	ductile	0.0038	0	no	0.0026
V-22Ti-2Fe	ductile	did not break	broke during test	yes	0
V-33Ni-33Ti	ductile	did not break	0	no	did not break
V-10Ni-5Al	ductile	failed hot rolling			
Nb-1Zr	ductile	> 0.0067	broke during test	yes, severely	
Cu-41Nb	ductile	0.0016	3.9×10^{-9}	yes	did not break
Ti-18Mo	ductile	> 0.0086			0

Table 2. Comparison of Important Parameters for Metal Membrane Materials

Alloy (at.%)	Thickness (mm)	Surface Coating	Temp. (°C)	Permeability ($mol/m \cdot s \cdot Pa^{0.5}$)	Activation Energy (kJ/mol)
V-10Pd	0.107	100 nm Pd	400	3.86×10^{-8} *	≥ 400°C: 12.9 kJ/mol < 400°C: 38.8 kJ/mol
V	0.375	100 nm Pd	400	3.62×10^{-7}	28.0
Pd-23Ag	0.250	NA	400	2.52×10^{-8}	10.8

*avg. of three different membranes

Table 3. Comparison of the Susceptibility of Various Membrane Materials to Hydrogen Embrittlement

Membrane Composition (at.%)	Thickness (mm)	Failure Temperature (°C)	Failure H_2 Pressure ΔP (kPa)
V (this work)	0.040	262	97
V [71]	0.040	300	326
V [45]	1	200	22.7
V-10Pd (this work)	0.107	118	97
Pd-23Ag (this work)	0.250	< 25	NA

Appendix: Some V and Nb alloys (at.%) that were too brittle to form membranes or embrittled severely in hydrogen so that permeability data could not be obtained

V-10Ni-9Co-1C	V-9.2Ni-7Mn-1.2C	V-10Mo-9Ru
V-14Ti-9Ni-8Co	V-8Ni-6Mn-1C	V-7Mo-7Ru
Ti-32V-19Co-8Ni	V-13Pd-6Ti	V-7Mo-6.6Ru-1.4C
Ti-30V-21Co-1C	V-9Ni-5Pd-4Ti	V-11Ti-6Mo-5Ru
V-11Ti-9Co-9Pd	V-9Ti-8Ni-5Pd	V-10Ti-5Ru-5Mo
V-7Fe	V-26Ti-7Ni-7Pd	V-35Ti-14Ni-13Al
V-7Ni-6Fe	V-38Ti-11Ni-7Pd	V-28.1Ti-21Ni-10Al
V-9.2Ni-5.1Pd-1.3C	Ti-32V-22Ni-9Pd	V-32Ni-24Ti-10Al
V-4Ru	V-32Ti-18Cr-C	V-34.1Ti-13.4Ni-12.8Al-1.2C
V-8Ru	V-40Ti-15Al	Co-34Ti-28V
V-14Ru	V-10Cu-5Pd	V-25Co-23Ti-10Ni
V-33Ru	V-8Cu-4Pd	V-31Co-24Ti
V-19Mn	V-6Cu-3Pd	Co-32V-30Ti
V-28Mn	V-5.7Cu-2.8Pd-1.3C	Co-30Ti-25V-12Ni
V-13Ni-10Mn	V-6Cu-3Pd-2Y	Co-29.6Ti-24.1V-12Ni-1.3C
V-10Ni-7Mn	V-5Cu-3Pd-3Y	V-30.2Co-24.2Ti-1.3C
V-9Ni-3Ti	V-20Mn-6Ru	Nb-13Pd
V-9Co	V-8Ru-6Ni	
V-10.1Ni-7.2Mn-1.3C	V-13Mo-12Ru	

References

1. T. M. Adams and J. Mickalonis: *Mater. Lett.*, 2007, **61**, 817-820.
2. A. Adrover, M. Giona, L. Capobianco, P. Tripodi, and V. Violante: *J. Alloys Compd.*, 2003, **358**, 157-167.
3. M. Amano, M. Komaki, and C. Nishimura: *J. Less-Common Met.*, 1991, **172-174**, 727-731.
4. A. Basile, F. Gallucci, A. Iulianelli, G. F. Tereschenko, M. M. Ermilova, and N. V. Orekhova: *J. Membr. Sci.*, 2008, **310**, 44-50.
5. N. Boes and H. Züchner: *Zeitschrift für Naturforschung A*, 1976, **31**, 754-759.
6. R. Burch and N. B. Francis: *J. Less-Common Met.*, 1976, **49**, 371-384.
7. R. E. Buxbaum: U.S. Patent 5,108,724, Nov. 27, 1991.
8. R. E. Buxbaum, P.C. Hsu: U.S. Patent 5,149,420, Sep. 22, 1992.
9. R. E. Buxbaum and P. C. Hsu: *J. Nucl. Mater.*, 1992, **189**, 183-192.
10. R. E. Buxbaum: U.S. Patent 6,576,350, Jun. 10, 2003.
11. R. E. Buxbaum and A. B. Kinney: *Ind. Eng. Chem. Res.*, 1996, **35**, 530-537.
12. J. P. Collins and J. D. Way: *Ind. Eng. Chem. Res.*, 1993, **32**, 3006-3013.
13. D. Demange, S. Welte, and M. Glugla: *Fusion Eng. Des.*, 2007, **82**, 2383-2389.
14. M. D. Dolan, N. C. Dave, A. Y. Ilyushechkin, L. D. Morpeth, and K. G. McLennan: *J. Membr. Sci.*, 2006, **285**, 30-55.

15. D. J. Edlund: 'Engineering Scale-up for Hydrogen Transport Membranes', in 'Nonporous Inorganic Membranes', (ed. A. F. Sammells and M. V. Mundschau), 139-164; 2006, Weinheim, Germany, Wiley-VCH.
16. D. J. Edlund and J. McCarthy: *J. Membr. Sci.*, 1995, **107**, 147-153.
17. C.-H. Fagerstroem, F. D. Manchester, and J. M. Pitre: 'H-V (Hydrogen-Vanadium)', in 'Phase Diagrams of Binary Hydrogen Alloys', (ed. F. D. Manchester), 273-292; 2000, Materials Park, Ohio, U.S.A., ASM Int.
18. V. M. Gryaznov: *Sep. Purif. Meth.*, 2000, **29**, 171-187.
19. K. Hashi, K. Ishikawa, T. Matsuda, and K. Aoki: *J. Alloys Compd.*, 2005, **404**, 273-278.
20. Y. Hatano, R. Hayakawa, K. Nishino, S. Ikeno, T. Nagasaka, T. Muroga, and K. watanabe: *Mater. Trans.*, 2005, **46**, 511-516.
21. Y. Hatano, K. Ishiyama, H. Homma, and K. Watanabe: *J. Alloys Compd.*, 2007, **446**, 539-542.
22. Y. Hatano, A. Livshits, A. Busnyuk, M. Nomura, K. Hasizume, M. Sugisaki, Y. Nakamura, N. Ohyabu, and K. Watanabe: *Phys. scr.*, 2004, **2004**, 14-18.
23. R. Hayakawa, Y. Hatano, A. Pisarev, and K. Watanabe: *Phys. scr.*, 2004, **T108**, 38-41.
24. G. L. Holleck: *J. Phys. Chem.*, 1970, **74**, 1957-1961.
25. R. C. Hurlbert and J. O. Konecny: *J. Chem. Phys.*, 1961, **34**, 655-658.
26. K. Ishikawa, W. Luo, and K. Aoki: *Mater. Res. Soc. Symp. Proc.*, 2006, **885**, 251-256.
27. D. Jewett and A. C. Makrides: 'Research studies on solid hydrogen purification membranes. Interim technical report No. 2, May 15-Nov 15, 1966', PB--230845 or AD650986, Tyco Labs Inc., Waltham, Massachusetts, 1967.
28. S. P. Kaldis, G. Skodras, and S. G.P.: *Fuel Processing Tech.*, 2004, **85**, 337-346.
29. H. Katsuta, R. B. McLellan, and K. Furukawa: *Proc. JIMIS-2. Hydrogen in Metals*, 1980, **21**, 113-116.
30. K. Komiya, S. Ito, H. Yukawa, M. Morinaga, K. Nagata, T. Nambu, and H. Ezaki: *Mater. Trans.*, 2003, **44**, 1686-1689.
31. A. J. Kumnick and H. H. Johnson: *Metall. Trans. A*, 1975, **6**, 1087-1091.
32. M. Lagos and I. Schuller: *Surf. Sci. Lett.*, 1984, **138**, L161-L167.
33. W. Luo, K. Ishikawa, and K. Aoki: *J. Alloys Compd.*, 2006, **407**, 115-117.
34. A. C. Makrides, M. A. Wright, D. N. Jewett: U.S. Patent 3,350,846, Nov. 7, 1967.
35. W. Mekonnen, B. Arstad, H. Klette, J. C. Walmsey, R. Bredesen, H. Venvik, and R. Holmestad: *J. Alloys Compd.*, 2008, **310**, 337-348.
36. J. Miyazaki, T. Kajiyama, K. Matsumoto, H. Fujiwara, and M. Yatabe: *Int. J. Hydrogen Energy*, 1996, **21**, 335-341.
37. T. S. Moss, N. M. Peachey, R. C. Snow, and R. C. Dye: *Int. J. Hydrogen Energy*, 1998, **23**, 99-106.
38. M. Mundschau, X. Xie, and A. F. Sammells: 'Hydrogen transport membrane technology for simultaneous carbon dioxide capture and hydrogen separation in a membrane shift reactor', in 'Carbon Dioxide Capture for Storage in Deep Geologic Formations', (ed. D. C. Thomas and S. M. Benson), 291-306; 2005, Elsevier, Ltd.

39. M. V. Mundschau, X. Xie, C. R. Evenson IV, and A. F. Sammells: *Catal. Today*, 2006, **118**, 12-23.
40. K. Nakamura, H. Uchida, and E. Fromm: *J. Less-Common Met.*, 1981, **80**, P19-29.
41. C. Nishimura, M. Komaki, and M. Amano: *Mater. Trans., JIM*, 1991, **32**, 501-507.
42. C. Nishimura, M. Komaki, S. Hwang, and M. Amano: *J. Alloys Compd.*, 2002, **330-332**, 902-906.
43. C. Nishimura, J. Y. Yang, and M. Komaki: *J. Alloys Compd.*, 2007, **431**, 180-184.
44. T. Ozaki, Y. Zhang, M. Komaki, and C. Nishimura: *Int. J. Hydrogen Energy*, 2003, **28**, 1229-1235.
45. T. Ozaki, Y. Zhang, M. Komaki, and C. Nishimura: *Int. J. Hydrogen Energy*, 2003, **28**, 297-302.
46. S. Paglieri and J. D. Way: *Sep. Purif. Meth.*, 2002, **31**, 1-169.
47. S. N. Paglieri: 'Palladium Membranes', in 'Nonporous Inorganic Membranes', (ed. A. F. Sammells and M. V. Mundschau), 77-105; 2006, Weinheim, Germany, Wiley-VCH.
48. S. N. Paglieri, I. E. Anderson, R. L. Terpstra, T. J. Venhaus, Y. Wang, R. E. Buxbaum, K. S. Rothenberger, and B. H. Howard: 'Metal membranes for hydrogen separation', 20th Annual Conf. Fossil Energy Mater., Knoxville, Tennessee, U.S.A., June 12-14, 236-243.
49. N. M. Peachey, R. C. Snow, and R. C. Dye: *J. Membr. Sci.*, 1996, **111**, 123-133.
50. T. P. Perng and C. J. Altstetter: *Metall. Trans. A*, 1986, **17**, 2086-2090.
51. M. A. Pick: *J. Nucl. Mater.*, 1987, **145-147**, 297-300.
52. F. Roa, J. D. Way, R. L. McCormick, and S. N. Paglieri: *Chem. Eng. J.*, 2003, **93**, 11-22.
53. K. S. Rothenberger, B. H. Howard, R. P. Killmeyer, A. V. Cugini, R. M. Enick, F. Bustamante, M. V. Ciocco, B. D. Morreale, and R. E. Buxbaum: *J. Membr. Sci.*, 2003, **218**, 19-37.
54. Y. Saito and Y. Fukai: *J. Less-Common Met.*, 1988, **138**, 161-172.
55. Y. Sasaki and M. Amano: 'Hydrogen solubility and embrittlement in Nb-V, Nb-Mo and Nb-Ta alloys', 2nd Int. Conf. on Hydrogen in Metals, Paris, France, Jun. 6-11, 3C3.
56. E. Serra, M. Kemali, A. Perujo, and D. K. Ross: *Metall. Mater. Trans. A.*, 1998, **29A**, 1023-1028.
57. J. Shu, B. P. A. Grandjean, A. Van Neste, and S. Kaliaguine: *Can. J. Chem. Eng.*, 1991, **69**, 1036-1060.
58. A. Sieverts and W. Krumbhaar: *Berichte der Deutsch Chemische Gesellschaft*, 1910, **43**, 893-900.
59. D. L. Smith, H. M. Chung, B. A. Loomis, H. Matsui, S. Votinov, and W. Van Witzenburg: *Fusion Eng. Des.*, 1995, **29**, 399-410.
60. J. F. Smith: 'Pd-V (Palladium-Vanadium)', in 'Binary Alloy Phase Diagrams', (ed. J. F. Smith), 3062-3065; 1989, Materials Park, Ohio, USA, ASM Int.
61. R. V. Steward, M. L. Grossbeck, B. A. Chin, H. A. Aglan, and Y. Gan: *J. Nucl. Mater.*, 2000, **283-287**, 1224-1228.
62. S. A. Steward: *US National Laboratory Report*, 1983, **UCRL-53441**.

63. C. L. Stokes and R. E. Buxbaum: *Nucl. Tech.*, 1991, **98**, 207-216.
64. R. A. Strehlow and H. C. Savage: *Nucl. Tech.*, 1974, **22**, 127-137.
65. T. Takeda, A. Ying, and M. A. Abdou: *Fusion Eng. Des.*, 1995, **28**, 278-285.
66. S. Tanaka and H. Kimura: *Proc. JIMIS-2. Hydrogen in Metals*, 1980, **21**, 513-516.
67. H. Tang, K. Ishikawa, and K. Aoki: *Mater. Trans.*, 2007, **48**, 2454-2458.
68. J. Tong, L. L. Su, Y. Kashima, R. Shirai, H. Suda, and Y. Matsumura: *Ind. Eng. Chem. Res.*, 2006, **45**, 648-655.
69. E. H. Van Deventer, T. a. Renner, R. H. Pelto, and V. A. Maroni: *J. Nucl. Mater.*, 1977, **64**, 241-248.
70. W. Weirich, B. Biallas, B. Kügler, M. Oertel, M. Pietsch, and U. Winkelmann: *Int. J. Hydrogen Energy*, 1986, **11**, 459-462.
71. S. Wieland, T. Melin, and A. Lamm: *Chem. Eng. Sci.*, 2002, **57**, 1571-1576.
72. J. Y. Yang, C. Nishimura, and M. Komaki: *J. Alloys Compd.*, 2007, **431**, 180-184.
73. D. Yepes, L. M. Cornaglia, S. Irusta, and E. A. Lombardo: *J. Membr. Sci.*, 2006, **274**, 92-101.
74. W.-S. Zhang and Z.-L. Zhang: *J. Alloys Compd.*, 2002, **346**, 176-180.
75. y. Zhang, R. Maeda, M. Komaki, and C. Nishimura: *J. Membr. Sci.*, 2006, **269**, 60-65.
76. Y. Zhang, T. Ozaki, M. Komaki, and C. Nishimura: *J. Membr. Sci.*, 2003, **224**, 81-91.

Figure 1. A typical composite membrane disc sealed between two Cu VCR gaskets (Ni gaskets are normally used). This 0.37-mm thick V-6Ni-5Co membrane (coated with 100 nm Pd per side) was tested for 170 h at 450°C.[48]

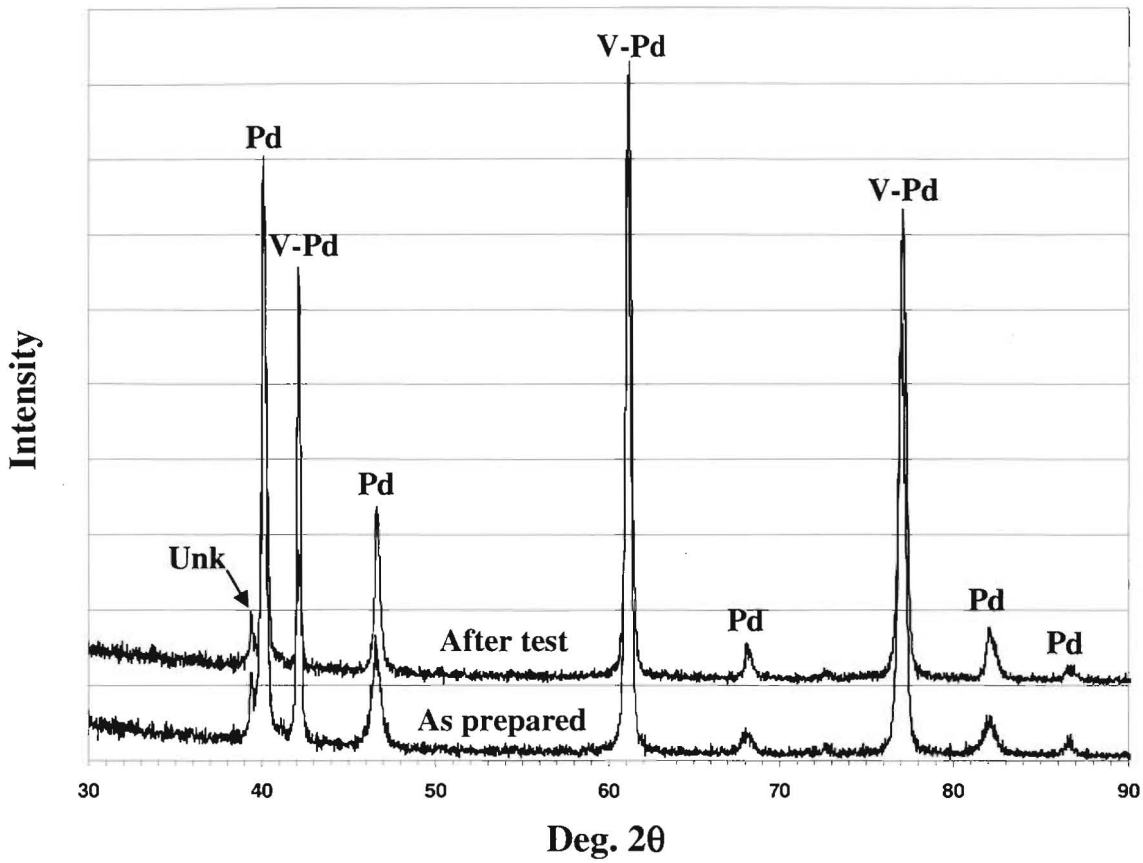

Fig. 2. XRD patterns for Pd-coated (100 nm) V-10Pd membranes before and after testing at 400°C for 162 h.

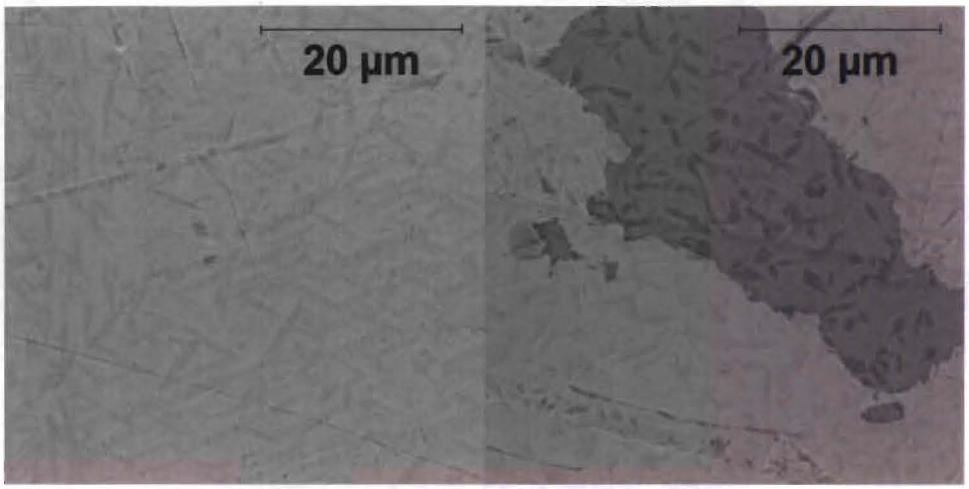

(a) (b)

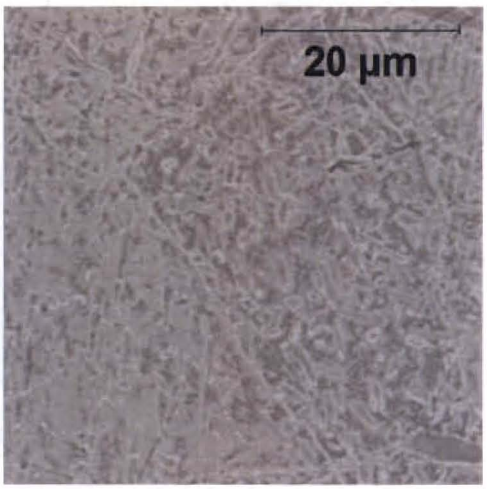

(c)

Fig. 3. Surface of the Pd-coated (100 nm) V-10Pd membrane before (a, b) and after (c) testing in hydrogen for 162 h at 400°C showing: the surface texture (a); a spot (< 2% of the total surface area) where Pd delaminated from the surface (b); and the increase in surface roughness during testing (c).

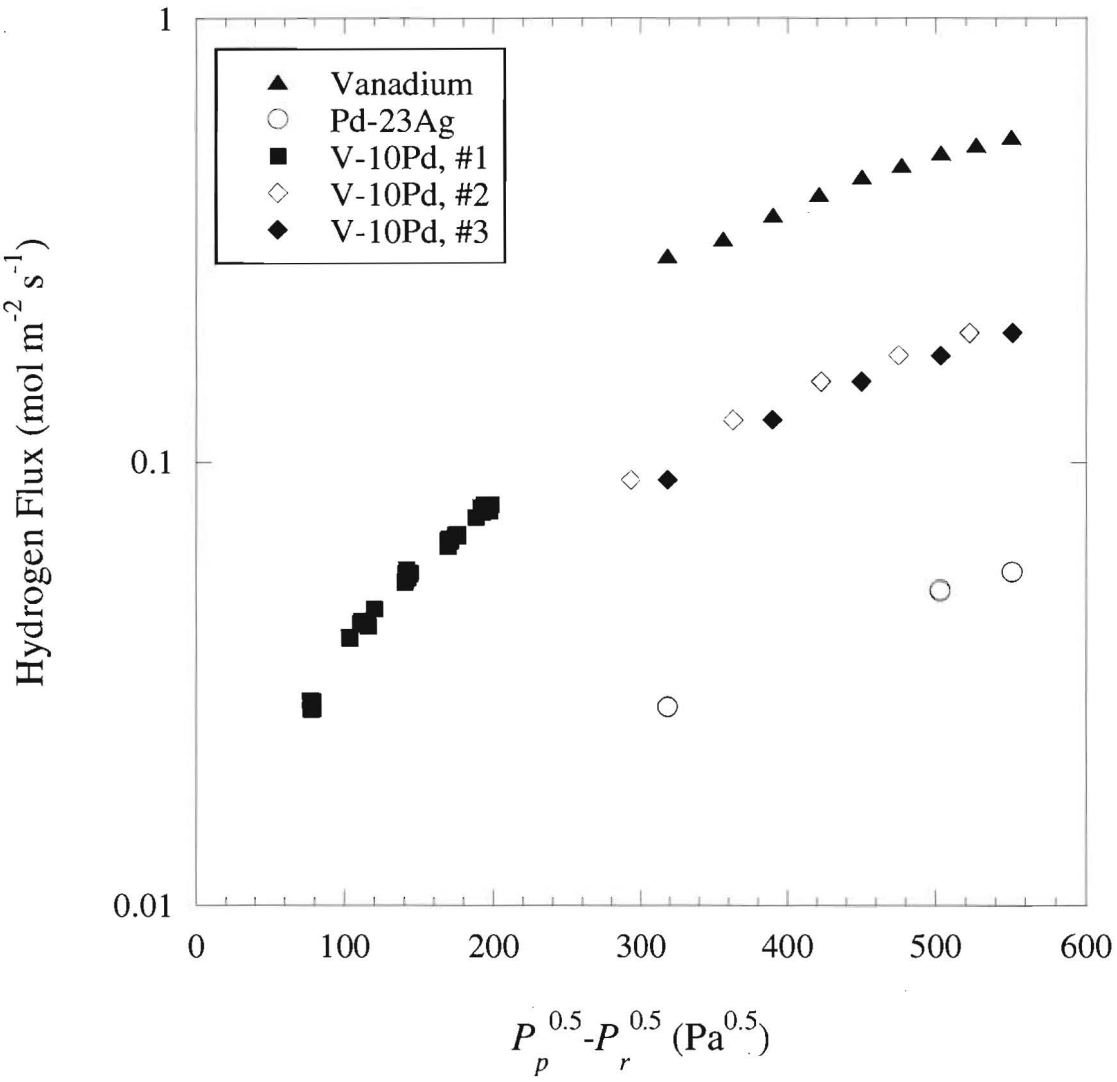

Figure 4. Hydrogen flux dependence on pressure at 400°C through three different samples of 0.107-mm-thick Pd-coated (100 nm) V-10Pd membrane, a Pd-coated (100 nm) 0.375-mm-thick V membrane, and a 0.250-mm-thick Pd-23Ag membrane.

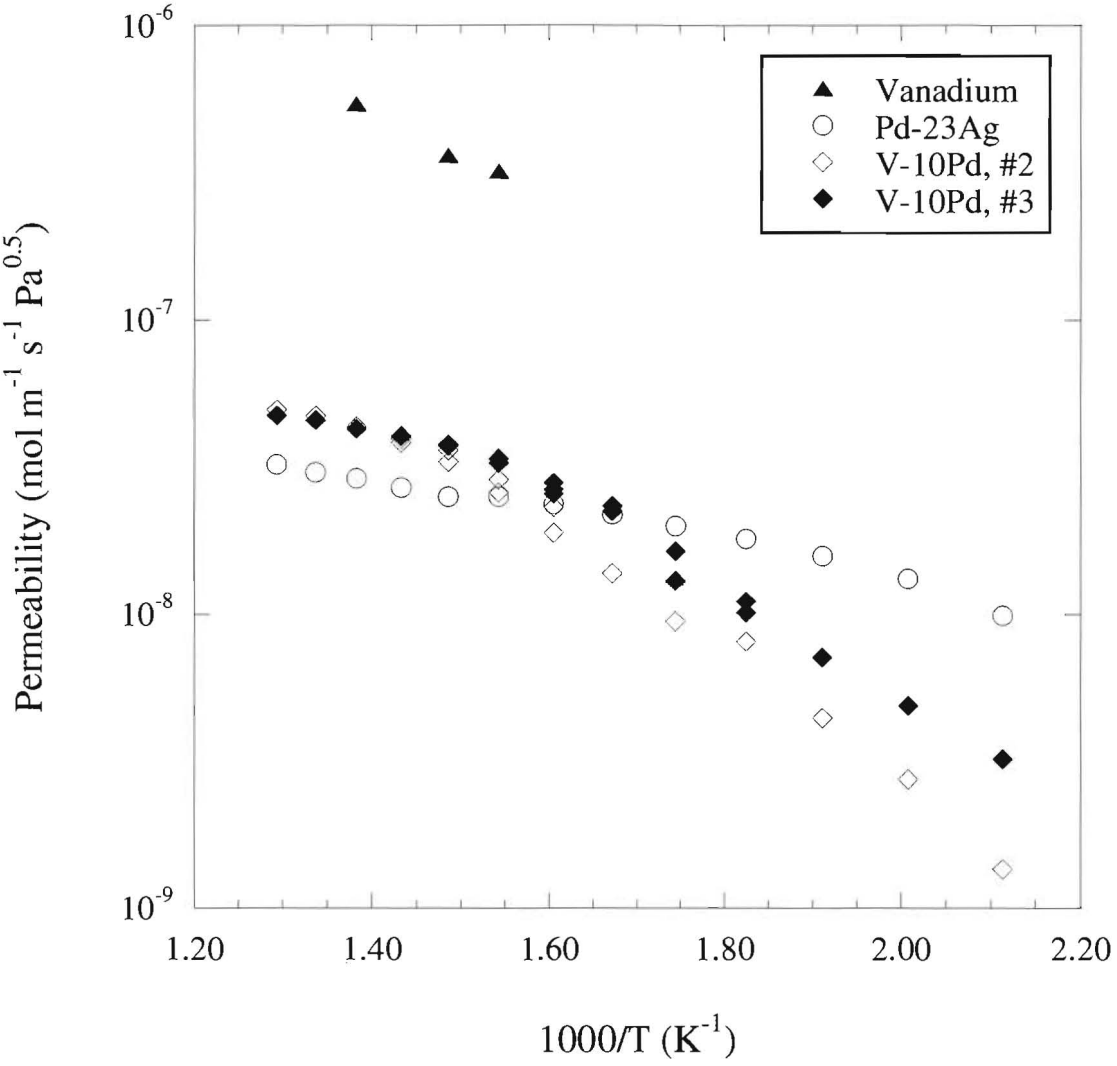

Figure 5. Temperature dependence of hydrogen permeabilities for Pd-coated (100 nm) V, two different Pd-coated (100 nm) V-10Pd membranes, and a Pd-23Ag membrane.

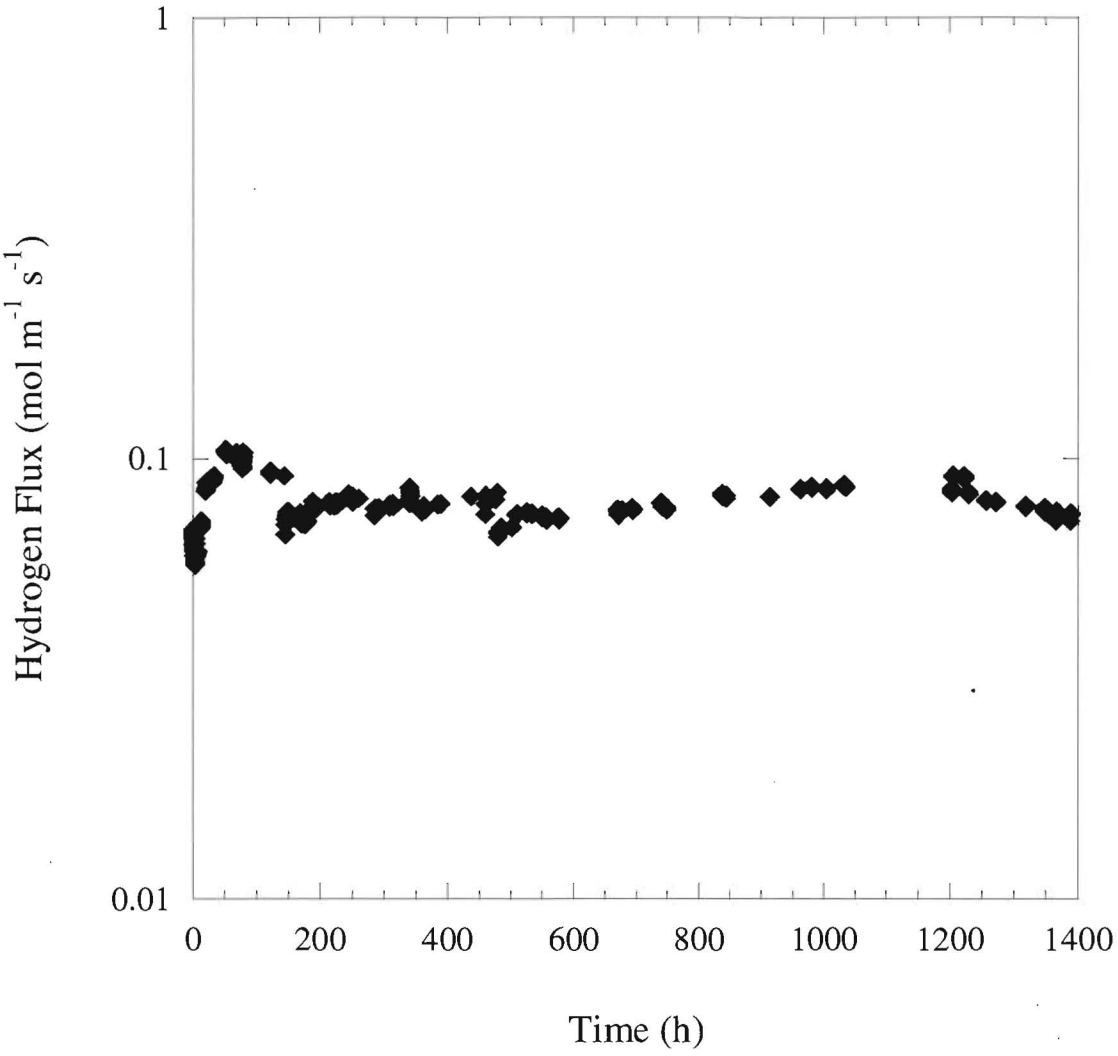

Figure 6. Long term hydrogen flux test for a 0.107-mm-thick Pd-coated (100 nm) V-10Pd membrane at 400°C. The pressure of hydrogen on the retentate side of the membrane was 101 kPa and the pressure on the permeate side was 0.6 kPa.